NUMERICAL MODELING OF LUNAR MULTI-RING BASINS

R. W. K. Potter[1], G. S. Collins[1], D. A. Kring[2] , W. S. Kiefer[2], P. J. McGovern[2], [1]Impacts and Astromaterials Research Centre, Dept. Earth Science and Engineering, Imperial College London, London, UK, ross.potter04@imperial.ac.uk; [2]Lunar and Planetary Institute, 3600 Bay Area Boulevard, Houston, TX, USA

Introduction: As the rarest impact structures in the Solar System, multi-ring basins are the least understood. Various hypotheses have been proposed to explain their formation and features [*e.g.* 1-3]. Currently scaling laws, based on measurements of smaller-scale craters, are used to estimate multi-ring basin attributes [*e.g.* 4]. Whether multi-ring basins follow this scaling is debated.

On Earth, possible multi-ring basins are either severely eroded (Sudbury, Vredefort) or buried (Chicxulub), making inferences of their original structure problematic. Earth's Moon however, has a relative abundance of multi-ring basins [5], making it a suitable location for the study of multi-ring basins [6].

Gravitational and topographic data over a number of lunar basins has been collected and crustal profiles inferred [7,8]. These data show basins possess a thinned crust beneath their centers and a thickened annulus of crust towards their rims. The largest basins may have excavated mantle material [8].

The majority of, if not all, lunar basins are thought to have formed during a Lunar Cataclysm which ended ~3.9 Ga [9], when the Moon's interior was far hotter than its current thermal state [10]. The extreme antiquity of these basins means many are heavily degraded and the proposed higher temperatures are likely to have accelerated modification processes such as viscous relaxation [11]; basins today are not necessarily representative of their original form.

In this work we compare our numerical impact model with observations of crustal structure beneath lunar basins to test our model and further understanding of basin formation.

Methods: The two dimensional iSALE hydrocode [12,13] was used to model lunar basin impacts. iSALE has been used to model terrestrial impacts at various scales (*e.g*. Chesapeake [14]; Chicxulub [15]), as well as lunar SPA-scale impacts [16].

Projectiles 40-120 km in diameter, with a velocity of 15 km/s (close to the lunar average of 18 km/s), were impacted vertically into an infinite half-space representing the lunar surface, consisting of a 60 km thick crust overlaying mantle. The simulations were terminated when the major crater-forming motions ceased. An ANEOS-derived equation of state for dunite [17] was used to model the mantle and the impactor. The Tillotson equation of state with parameters derived for gabbroic anorthosite [18] was used to model the crust.

Material strength and thermal parameters were derived from fits to experimental rock strength data [19-22]. Two different thermal profiles (TP) estimating early lunar conditions, based on those of [16], were investigated. TP 1 had a near-surface temperature gradient of 10 K/km with a ~1670 K deep adiabatic temperature; TP 2 had a near-surface temperature gradient of 34 K/km with a ~1770 K deep mantle adiabatic temperature. Temperature was bounded by the solidus, so that mantle temperatures never exceeded the ambient melt temperature. Based on the thermal profiles, self-consistent pressure, density and strength fields were computed. The gravity field was set to a constant value of 1.63 m/s^2. A constant resolution of 20 cells per projectile radius, CPPR, (cell sizes of 1-3 km) was used for all simulations.

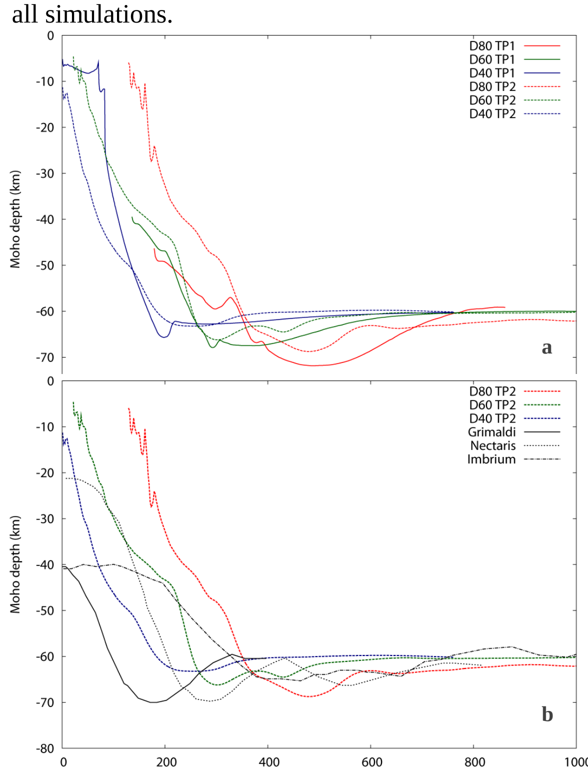

Figure 1. a) Final crustal profiles for lunar impacts of different sizes (D = impactor diameter) and for two different thermal profiles. The Moho is plotted from the innermost occurrence of crustal material to 1000 km radius **b)** Selected crustal profiles based on gravity modeling [7] are plotted against model results for thermal profile TP 2.

Results: Figure 1a shows the final Moho (crust/mantle boundary) profile for models with different impactor sizes and thermal profiles. For impactors 60 km in diameter or larger crustal material is completely removed from the basin center, creating a central pool of molten mantle; the diameter of which increases as impactor diameter increases. From its innermost occurrence, crust thickens away from the basin center, forming an annulus of thickened crust then thinning to pre-impact level outside the crater, qualitatively consistent with gravity-derived crustal profiles (Fig 1b). The radius and amplitude of the maximum in crustal thickness increases with increasing impactor size. In addition, maximum crustal thickness is smaller for impacts into a hotter lunar surface (TP 2 vs TP 1).

Figure 2 shows the relationship between thinned crust radius (distance from basin center to maximum crustal thickness) and Moho uplift (uplift of base of crust at crater center as a fraction of pre-impact crustal thickness; 1 implies complete removal of crust). Observational data [7,8] show a maximum in Moho uplift of 0.8-1 at a thinned crust radius of 300 km; above this, Moho uplift appears to decreases. In contrast, our model results suggest Moho uplift increases to 1 at a thinned crust radius of ~300 km at remains at 1 for all larger craters.

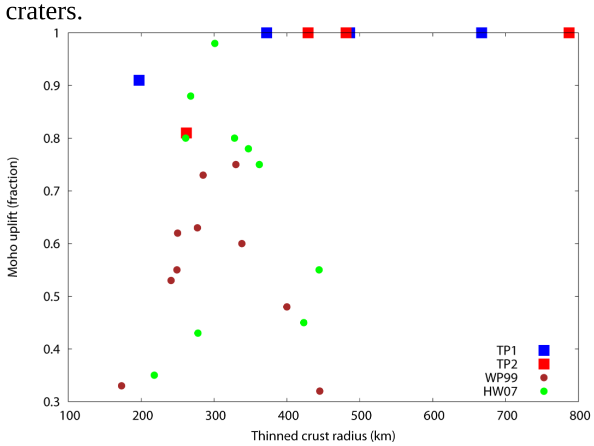

Figure 2. Moho uplift as a function of thinned crust radius. Observational data (WP99 [7], HW07 [8]) appear to show a decrease in Moho uplift beyond a thinned crust radius of 300 km. (The largest basins plotted are Imbrium and Serenitatis.) Our results show Moho uplift remains at 1 beyond this.

Discussion: Our preliminary results suggest, for vertical impacts at 15 km/s, impactors greater than ~60 km in diameter completely remove crustal material from the basin center, replacing it with a central melt pool of a predominantly mantle source. Hence, the crustal profiles beneath our final modeled craters contradict interpretations of gravity data that show a continuous crustal layer under all lunar basins [7]. However, more recent lunar spectral and crustal data from the better resolved and wider coverage of Kaguya suggests that mantle material could have been excavated in a number of basin-forming impacts as crustal thickness below some basins appears minimal [23] and possible mantle-derived olivine-rich signatures are present [24]. Model and observational differences can be reconciled if the mantle melt pool predicted by our models differentiated, forming a new crustal layer. As melt volume increases in proportion to crater volume with increasing crater size, the thickness of the crust formed by melt pool differentiation is expected to increase with crater size, explaining the apparent decrease in Moho uplift with crater size (Fig. 2). [7,8] suggest the small Moho uplift in the largest two basins (Imbrium, Serenitatis) is caused by significant basin relaxation due to their proximity to the thermally hot Procellarum KREEP Terrane. Crustal profiles beneath large lunar basins based on observational data suggest that maximum crustal thickness decreases with increasing crater size (Fig. 1b). For a given thermal profile, our model results suggest the opposite trend. As our models also show that maximum crustal thickness is smaller for a warmer thermal profile, this apparent discrepancy might be explained by the fact that (on average) smaller basins formed later than larger basins when the lunar interior was cooler.

Acknowledgements: We are grateful to Boris Ivanov, Jay Melosh, Kai Wünneman and Dirk Elbeshausen for their work in the development of iSALE. GSC was funded by NERC grant NE/E013589/1.

References: [1] Head, J.W. (1974) *The Moon*, 11, 327-356 [2] Melosh, H.J. & McKinnon, W.B. (1978) *GRL*, 5, 985-988 [3] Brittan, J. et al (1999) In: *GSA Spec. Pap*. 339, 269-280 [4] Cintala, M.J. & Grieve, R.A.F. (1998) *MAPS*, 33, 889-912 [5] Wilhelms, D.E. (1987) *The Geological History of the Moon*, U.S. Government Printing Office, Washington, D.C. [6] NRC (2007) *The Scientific Context for the Exploration of the Moon*, National Academies Press, Washington, D.C. [7] Wieczorek, M.A. & Phillips, R.J. (1999) *Icarus*, 139, 246-259 [8] Hikida, H. & Wieczorek, M.A. (2007) *Icarus*, 192, 150-166 [9] Tera, F. et al (1974) *EPSL*, 22, 1-21 [10] Shearer, C.K. et al (2006) *Revs. Min. Geochem*., 60, 365-518 [11] Mohit, P.S. & Phillips, R.J. (2006) *JGR*, 111, E12001 [12] Amsden, A.A. et al (1980) *Los Alamos National Laboratory Report LA-8095* [13] Collins, G.S. et al (2004) *MAPS* 39, 217-231 [14] Collins, G.S. & Wünneman, K. (2005) *Geology*, 33, 925-928 [15] Collins, G.S. et al (2008) *EPSL*, 270, 221-230 [16] Potter, R.W.K. et al. (2010) *LPSC XLI*, #1700 [17] Benz, W. et al (1989) *Icarus*, 81, 113-131 [18] O'Keefe, J.D. & Ahrens, T.J. (1982) *Geol. Soc. Am. Spec. Pap. 190* **[**19] Azmon, E. (1967) *NSL 67-224* [20] Stesky, R.M. et al (1974) *Tectonophys.*, 23, 177-203 [21] Shimada, M. et al (1983) *Tectonophys*., 96, 159-192 [22] Ismail, I.A.H. & Murrell, S.A.F. (1990) *Tectonophys*., 175, 237-248 [23] Ishihara, Y. et al (2009) *GRL*, 36, L19202 [24] Yamamoto, S. et al (2010) *Nature Geoscience*, 3, 533-536